MODELING RUBBLE-PILE IMPACTS: SPHERES VS. POLYHEDRA. D. G. Korycansky, *CODEP, Department of Earth and Planetary Sciences, University of California, Santa Cruz CA 95064 (kory@pmc.ucsc.edu).*

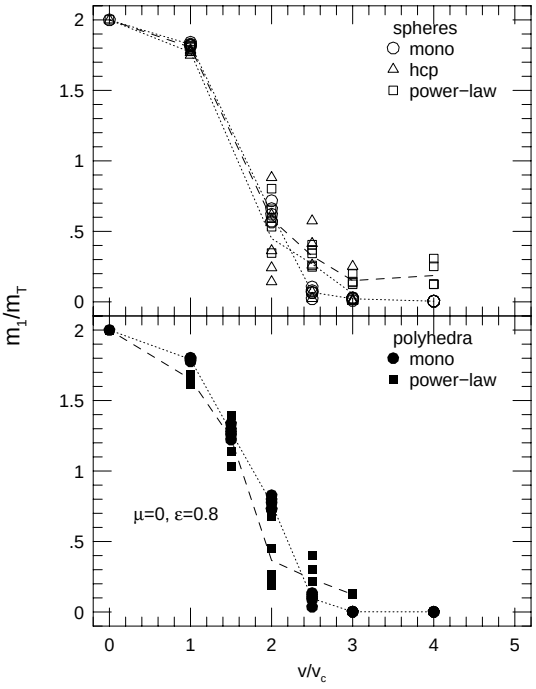

Figure 1: Mass ratio m_1/m_T of largest fragments versus scaled impact velocity v/v_c for low-dissipation (LD) runs ($\mu = 0$, $\varepsilon = 0.8$). Top: results for spherical elements: initial impact and targets of randomly packed monodisperse spheres (circles), hexagonal close-packing (triangles), and randomly-packed spheres from a power-law distribution (squares). Bottom: results for polyhedral elements: monodisperse (circles) and power-law mass distribution (squares).

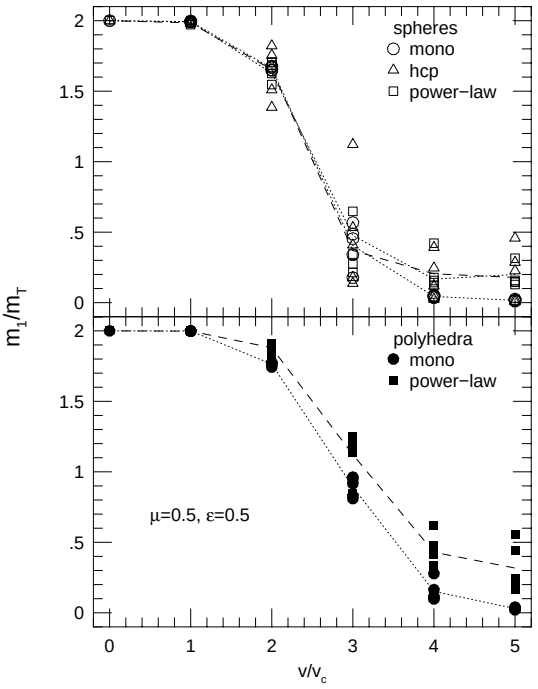

Figure 2: Mass ratio m_1/m_T of largest fragments versus scaled impact velocity v/v_c for high-dissipation (HD) runs ($\mu = 0.5$, $\varepsilon = 0.5$). Top: results for spherical elements: initial impact and targets of randomly packed monodisperse spheres (circles), hexagonal close-packing (triangles), and randomly-packed spheres from a power-law distribution (squares). Bottom: results for polyhedral elements: monodisperse (circles) and power-law mass distribution (squares).

A number of groups (e.g. [1-7]) have presented work modeling collisions between rubble-pile planetesimals and other interactions. For the most part, such computations have involved spherical sub-elements. Work by Korycansky [8] and Korycansky and Asphaug [9-11] by contrast, has made use of polyhedral elements that may provide potential for greater realism, as arbitrary shapes can be represented by the interacting elements. Our most recent calculations employ a so-called "physics engine"; a library of routines that simulate rigid body dynamics and include efficient methods for detecting and resolving collisions among non-spherical objects, a highly non-trivial problem [12]. Our choice of physics engine is the Open Dynamics Engine (ODE), a freely-available open-source package (`www.ode.org`). ODE includes a model for inelastic collisions and Coulomb frictional collisions, controlled by coefficients ε of restitution and friction μ. ODE can model objects of different shapes, including spheres and polyhedra with triangular faces.

The question arises: does object shape make any differ-

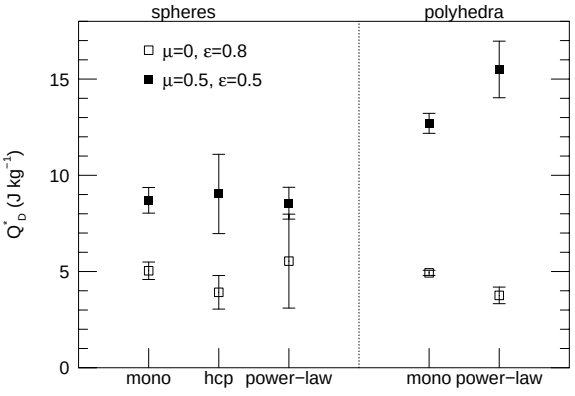

Figure 3: Critical disruption kinetic energy per unit mass Q_D^* for the various cases: monodisperse randomly-packed spheres, hexagonal close-packed spheres, power-law randomly-packed spheres, monodisperse polyhedra, and power-law polyhedra.

ence in the results of simulations? That is, are the results of calculations dependent on the shapes of the sub-elements that are employed in the calculations? We investigated this question for the case of 1 km diameter rubble piles colliding at modest speeds ($1-10$ m s^{-1}). In particular, we carried out a series of calculations of impacts at various speeds and measured the critical disruption energy per units mass Q_D^*, for which the mass m_1 of the largest fragment equals 1/2 the mass of the target m_T. We compared the outcomes of collisions of impactors and targets made of aggregates of spherical elements ("sphere objects") to those made of polyhedral elements ("polyhedron objects"). In the calculations reported here, the mass of the impactor $m_i = m_T$ and all collisions were head on (impact parameter $b = 0$) with no initial rotation of impactor or target. All simulations were carried out with $n = 1000$ elements in both impactor and target for a total of 2000 elements in each calculation. We ran a total of ~ 140 calculations for the sphere cases, and a subset of ~ 110 polyhedra calculations from Korycansky and Asphaug [11] was used for the comparison.

We looked at two sets of runs: "low-dissipation" (LD) in which the coefficients of friction and restitution were $\mu = 0.0$ and $\varepsilon = 0.8$, and "high-dissipation" (HD) for which $\mu = 0.5$ and $\varepsilon = 0.5$. Additionally, we investigated different arrangements and mass distributions in the impactors and targets: a "monodisperse" (single-mass) distribution and a power-law distribution for which the number of objects $N(>m)$ with mass greater than m was proportional to m^{-1}. For the sphere calculations, the monodisperse objects were either randomly packed or were made from hexagonal close-packed arrays ("hcp"). For each parameter set we ran five calculations in which the mutual orientation of the impactor and target was randomly chosen, so as to sample the stochasticity of the process. Impact velocities were scaled in terms of $v_c = M(6G/5\tilde{\mu}R)^{1/2}$, where $M = m_i + m_T$ and $\tilde{\mu} = m_i m_T/(m_i + m_T)$ is the reduced mass. For the objects described here, $v_c = 2.02$ m s^{-1}.

Results for LD and HD cases are shown in Figs. 1 and 2, respectively. The open symbols in the the top panels are for the various sphere cases, and the filled symbols in the bottom panels for the polyhedra runs. The results as expected are qualitatively similar for both kinds of objects. However, a closer look reveals some quantitative differences, particularly for the high-dissipation case.

Given the results shown in Figs 1 and 2, we can interpolate to find the velocity and hence kinetic energy Q_D^* for critical disruption. The results are given in Table 1. The error bars reflect the variance of the results in Figs. 1 and 2. In Fig. 3, we display Q_D^* for the various kinds of rubble pile and dissipation. From Fig. 3 we see that in the low dissipation case, there does not seem to be a systematic difference in Q_D^* between the sphere and polyhedron runs. Nor does there seem to be a systematic difference in results with respect to the sub-element arrangement (monodisperse, hcp, power-law). On the other hand, for the high dissipation runs, a significant difference is apparent. The polyhedron objects require $\sim 60\%$ more kinetic energy to disrupt compared to the sphere objects. Our tentative interpretation is the difference in the results is due to the presence of friction ($\mu \neq 0$) in the high dissipation case, whereas there is no friction in the low dissipation runs. However, the restitution coefficient ε is also different in the two cases, and that may also play a role. For the polyhedron objects we have also run a number of "medium dissipation" cases ($\mu = 0$, $\varepsilon = 0.5$), but at the time of writing there are not enough sphere runs completed to make a comparison. A final result of note is that in general, the dispersion (stochasticity) of the individual runs at a given impact velocity seems to be larger for the sphere objects as opposed to the polyhedron objects.

Table 1: Q_D^* for impact calculations (J kg^{-1})

	spheres			polyhedra	
	mono	hcp	p-law	mono	p-law
LD	5.0 ± 0.5	3.9 ± 0.9	5.5 ± 2.4	4.9 ± 0.1	3.8 ± 0.4
HD	8.7 ± 0.7	9.0 ± 2.1	8.6 ± 0.8	12.7 ± 0.5	15.5 ± 0.2

Acknowledgments

This work is supported by the NASA's Planetary Geology and Geophysics Program, under award NNX07AQ04G.

References

[1] Richardson and Bottke 1998, *Icarus*, **134**, 47. [2] Leinhardt *et al.* 2000, *Icarus*, **146**, 133. [3] Leinhardt and Richardson 2002, *Icarus* **159**, 306. [4] Leinhardt and Richardson 2005, *Astrophys. J.*, **625**, 427. [5] Stewart and Leinhardt 2008, *Astrophys. J. Lett.*, submitted. [6] Walsh and Richardson 2006, *Icarus*, **180**, 201. [7] Walsh and Richardson 2008, *Icarus*, **193**, 553. [8] Korycansky 2004, *Astrophys. Space Sci.* **291**, 57. [9] Korycansky and Asphaug 2006, *Icarus* **181**, 605. [10] Korycansky and Asphaug 2009, this conference. [11] Korycansky and Asphaug 2008, *Icarus*, submitted. [12] Baraff 1997. *An introduction to physically based modeling.* On-line lecture notes.